20.4 Design Solutions for a Multi-Object Wireless Power Transmission Sheet Based on Plastic Switches

Makoto Takamiya[1], Tsuyoshi Sekitani[1], Yoshio Miyamoto[1], Yoshiaki Noguchi[1], Hiroshi Kawaguchi[2], Takao Someya[1], Takayasu Sakurai[1]

[1]University of Tokyo, Tokyo, Japan, [2]Kobe University, Kobe, Japan

Wireless power delivery to electronic objects scattered over tables, walls and ceilings will form an infrastructure necessary for ubiquitous electronics, wireless sensor networks and ambient intelligence. Described here are design innovations to overcome the shortcomings of a previous wireless power transmission sheet [1] made with plastic MEMS switches and organic FETs (OFET) circuits suitable for printable low-cost electronics. The sheet delivers power to multiple objects, frees the users from position adjustment, reduces the number of coil arrays, and takes 5V digital input by using a newly developed level shifter.

The principle of wireless power transmission is based on an array of coils (TX-coil) made on a plastic sheet, which is selectively driven by plastic MEMS switches and is coupled magnetically with a receiver coil (RX-coil) mounted on a power receiving object as shown in Fig. 20.4.1. The MEMS switch can transfer amperes of current but the number of life-time switching cycles is limited up to 10^6 and the switching speed is as slow as a little less than a second. The selective TX-coil activation of small coils is needed for high power efficiency since if the RX-coil is made with one large coil, the coupling coefficient is decreased by a factor of one thousand in some cases. Position detection of the receiving object is needed for the selective activation of TX-coils. The position detection is carried out by OFETs as shown in Fig. 20.4.2, since scanning through many TX-coils to check if an RX-coil exists above a TX-coil by means of impedance change needs a faster speed and longer life-time than the MEMS switches.

As the sheet size gets large, power transmission at multiple random points on the sheet is required to deliver power to multiple objects and/or to deliver large power to a single object by using multiple RX-coils. In order to enable the multiple selection of TX-coils, conventional row and column decoders, which can select only one line at a time, are not sufficient. Thus, multiple line selection using an OFET SRAM [2] as shown in Fig. 20.4.2 is adopted. At first, all SRAMs are reset to "L". Then, only columns and rows above which RX-coils exist are selected. Multiple columns and rows can be selected simultaneously. By integrating the SRAMs and the decoders [3] on the OFET sheet, the number of the connections with off-sheet wires is decreased from 2N to $2log_2$N for an array of N×N coils.

Position adjustment-free power transmission is made possible by the following design. As shown in Fig. 20.4.1, the TX-coils are placed regularly with a pitch of 25.4mm which is called one unit. In [1], the TX-coils and the RX-coils have the same outer diameter (= 1 unit). In this case, as shown in Fig. 20.4.3(c), the power transmission efficiency changes from 58% to 2% with a displacement from 0 to 0.5 unit. Thus, 0.5-unit displacement is not allowed. This suggests a need for the exact positioning of the power receiving object. On the other hand, Fig. 20.4.3(a) shows the multiple activation technique of TX-coils, which tolerates the displacement. The outer diameter of the RX coils is set twice as large as that of the TX-coils. Figs. 20.4.3(b) and (c) show the measurement setup for the power transmission efficiency and the measured dependence of efficiency on the displacement of the RX-coil center to the TX-coil center with changing the number of activated TX-coils. It is seen that the efficiency becomes relatively insensitive to the displacement by using multiple TX-coil activation. Figure 20.4.3(d) shows the dependence of the maximum, average, and minimum power efficiency varied over the displacement amount on the number of activated TX-coils. The minimum efficiency achieves a maximum at 3×3 coils activation, which is considered to be the best design choice, because the minimum

efficiency determines the specification of the power transmission sheet. The proposed technique frees users from tedious position adjustment.

In contrast to [1], the circuit shown in Fig. 20.4.4(a) is devised by using two different frequencies and carefully eliminating interference of the two functions: the power transmission and the position detection. The circuit makes use of the fact that the conductivity of MEMS switches is more than 10^3 higher than that of OFETs. Thus, the OFET does not degrade the power transmission efficiency by shorting two frequency signal sources. C_1 is added to decrease the impedance at 13.56MHz (power transmission frequency) to improve the power efficiency while monitoring the impedance change for 3.5MHz (position detection frequency). C_P is added to increase the position detection sensitivity by peaking the impedance by LC resonance. As shown in Fig. 20.4.4(b), the measured resonant frequency of V_{MON} for the position detection system is around 8MHz to 10MHz, which is beyond the cutoff frequency of OFETs (3.5MHz). As seen from Fig. 20.4.4(b), in order to increase the sensitivity for the position detection, the higher the frequency used for position detection the better. Thus 3.5MHz is chosen as the frequency for the position detection. Figures 20.4.5(a) and (b) show the measured sensitivity for the position detection and power transmission efficiency, respectively. A 33% swing voltage change of V_{MOM} is observed between the two cases of with and without a RX-coil, and a 50% power transmission efficiency is achieved.

The integration of the silicon LSIs, OFETs, and MEMS devices is necessary in this power transmission system. Direct digital drive of OFETs and MEMS by silicon LSIs is, however, difficult, because there is a large discrepancy in the operation voltage between LSIs (below 5V) and OFETs/MEMS (above 40V). OFET level-shifters from 5V to 40V are developed as shown in Fig. 20.4.6. The basic topology of the shifter is a single amplifier whose gain depends strongly on the input level and thus adaptive biasing to adjust the input level with the source follower is preferable. A replica circuit is used for the adaptive biasing of the source follower in order to obtain the high voltage swing gain of the 5V input. The differential amplifier is a key circuit for the feedback control. It is, however, difficult to design a high-gain differential amplifier with only pMOS FETs in organic circuit design, because the impedance of a conventional organic pMOS load [4] is low. Figure 20.4.6 shows the proposed differential amplifier with enhancement/depletion mixed threshold voltages realized by controlling the back-gate voltage [5]. The load transistors M4 and M5 are of the depletion type and have higher impedance than the conventional topology because the gate and source are tied (off-connection if it is an enhancement FET). Figure 20.4.7(a) shows the measured characteristics for the differential amplifier. A gain of 6.4 is achieved, which is higher than 2.3 for the organic analog amplifier reported in [4]. Figure 20.4.7(b) shows the measured successful operation of the feedback control. Figures 20.4.7(c) and (d) show the measured DC and AC characteristics for the cascaded source follower and the single amplifier, respectively. The DC gain is measured to be 2.6 and the measured bandwidth is 430Hz.

References:
[1] T. Sekitani, et al., "A Large-Area Flexible Wireless Power Transmission Sheet Using Printed Plastic MEMS Switches and Organic Field-Effect Transistors," *presented at IEDM 2006.*, Dec., 2006.
[2] M. Takamiya, et al., "An Organic FET SRAM for Braille Sheet Display with Back Gate to Increase Static Noise Margin," *ISSCC Dig. Tech. Papers*, pp. 276-277, Feb., 2006.
[3] T. Someya, H. Kawaguchi, and T. Sakurai, "Cut-and-Paste Organic FET Customized ICs for Application to Artificial Skin," *ISSCC Dig. of Tech. Papers*, pp. 288-289, Feb., 2004.
[4] N. Gay, et al., "Analog Signal Processing with Organic FETs," *ISSCC Dig. Tech. Papers*, pp. 278-279, Feb., 2006.
[5] S. Iba, et al., "Control of Threshold Voltage of Organic Field-Effect Transistors with Double Gate Structure," *Applied Physics Letters*, 87, 023509, July 2005.
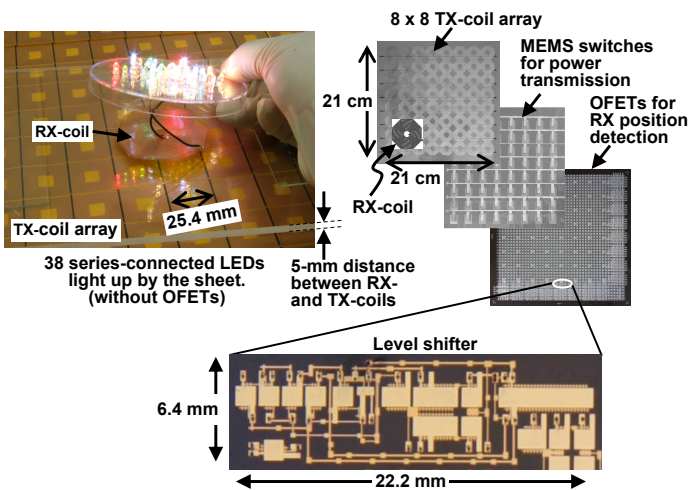
Figure 20.4.1: Wireless power transmission sheet.
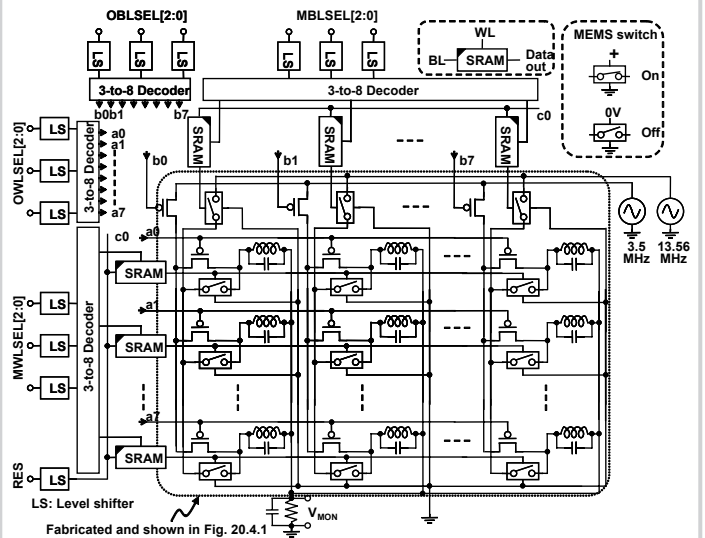
Figure 20.4.2: Circuit diagram of wireless power transmission sheet.
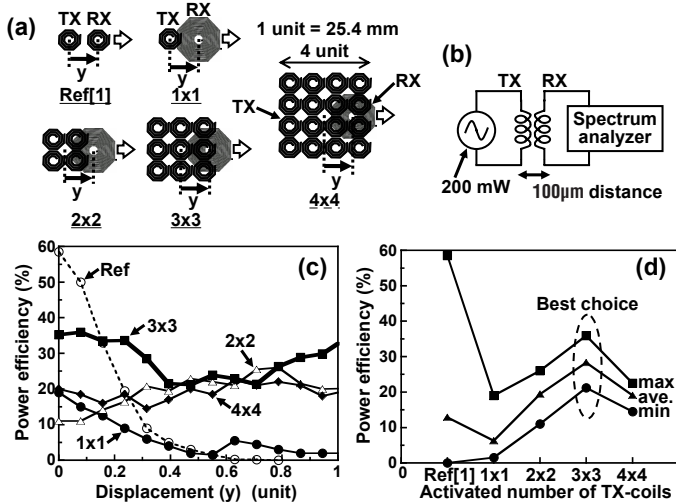
Figure 20.4.3: (a) Various arrangement of TX-coils and RX-coils. (b) Measurement setup. (c) Measured power efficiency dependence on displacement (y). (d) Power efficiency dependence on number of activated coils.
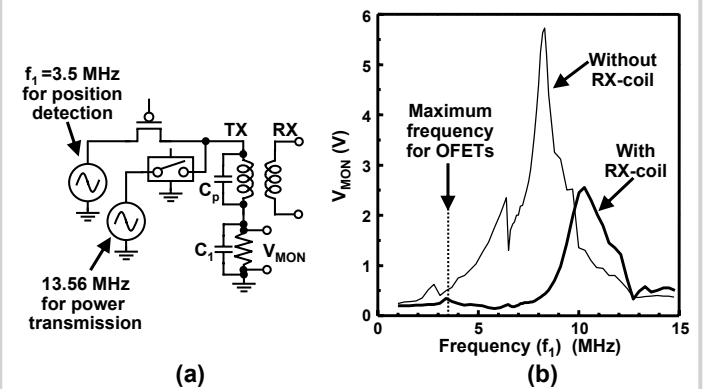
Figure 20.4.4: (a) Circuit diagram to share one TX-coil for power transmission and position detection. (b) Measured frequency response of monitored voltage (V_{MON}).
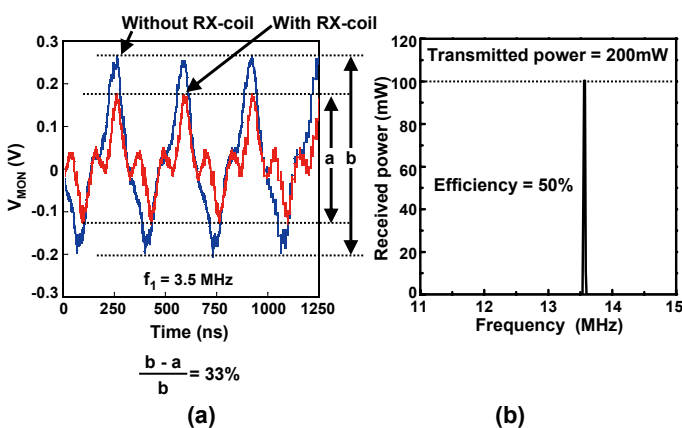
Figure 20.4.5: (a) V_{MON} waveform to show that 33% amplitude change is observed with and without RX-coil. (b) Measured received power spectrum.
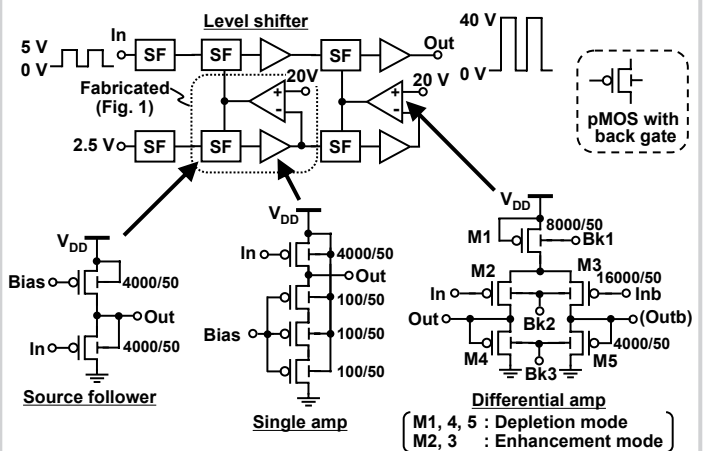
Figure 20.4.6: Circuit diagram of level shifter based on organic analog circuits with adaptive biasing and feedback loop.

20
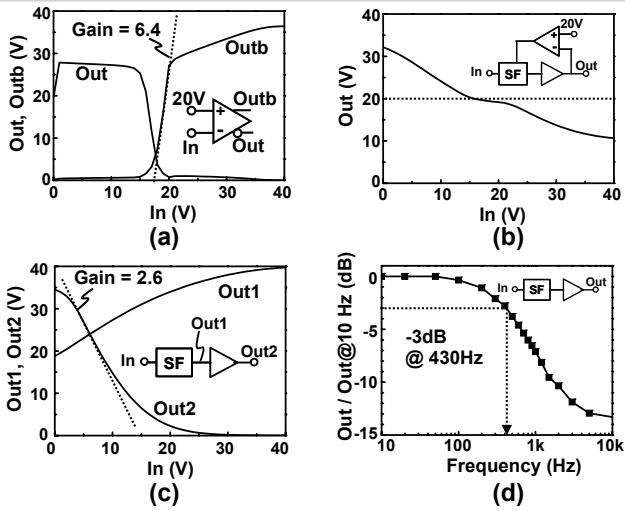
Figure 20.4.7: Measured results of level shifter. (a) DC characteristics of differential amplifier. (b) Feedback control. (c)(d) DC and AC characteristics for cascaded source follower and single amplifier respectively.